

Article

Evaluation of the Effect of Nd Content and Extrusion Process on Thermal Conductivity of Mg-Mn-Zn-Nd Alloys

Ying-Long Zhou ^{1,*}, Jie Liu ¹, Dong-Mei Luo ² and Dong-Chu Chen ³

¹ Department of Mechatronics Engineering, Foshan University, Foshan 528000, Guangdong, China; jie.liu.jdxy@fosu.edu.cn

² Department of Civil Engineering, Foshan University, Foshan 528000, Guangdong, China; dmluo@fosu.edu.cn

³ Department of Materials Science and Engineering, Foshan University, Foshan 528000, Guangdong, China; cdcever@163.com

* Correspondence: ylzhou@fosu.edu.cn

Received: 30 September 2018; Accepted: 6 November 2018; Published: 14 November 2018



Abstract: The thermal conductivity of the Mg-1Mn-2Zn-xNd alloys ($x = 0.5, 1.0, 1.5$ wt. %) was studied for the potential applications of heat dissipation. The phase constituents were examined by X-ray diffraction analysis, and the microstructure was observed by light and scanning electron microscopes. The thermal conductivity of the Mg alloys was gauged at room temperature using laser flash method. The experimental results indicate that the thermal conductivity of both the cast and extruded Mg alloys decreases slowly with Nd content, and the extrusion process remarkably reduces the grain sizes and thermal conductivity of the Mg alloys. The thermal conductivity of cast Mg-1Mn-2Zn-xNd alloys exceeds the required critical value ($100 \text{ W}/(\text{m}\cdot\text{k})$) for the cast Mg alloys. Among them, the cast Mg-1Mn-2Zn-1Nd alloy has great potential to be a good candidate of heat dissipation materials due to its good combination of thermal and mechanical properties.

Keywords: Mg alloy; microstructure; extrusion process; thermal conductivity; heat dissipation

1. Introduction

The rapid development of various electronic devices demands higher heat dissipation performance of metal fins. Silver, gold, copper and aluminum (Al) have the best thermal conductivity (427, 315, 398 and $237 \text{ W}/(\text{m}\cdot\text{K})$ for silver, gold, copper and Al at room temperature, respectively) among the metallic materials [1] and they should be expected to be good candidates of heat dissipation materials. Silver and gold, however, are precious metals with very high price, and copper also has its own disadvantages: high cost, large weight and poor corrosion resistance. This is the reason why the light Al alloys are often used to manufacture the most currently-used heat sinks. Recently, Magnesium (Mg) and its alloys have attracted a great attention as potential heat dissipation materials because Mg has good thermal conductivity of $156 \text{ W}/(\text{m}\cdot\text{K})$ at room temperature, which is only lower than that of pure Al among the commercially-used metallic materials [1], and it has much lower density (about $1.8 \text{ g}/\text{cm}^3$) and higher specific heat capacity as compared with the above metals. Pure Mg, however, has poor strength (about 21 MPa for cast Mg). The cast Mg alloys have much higher strength than pure Mg due to solution strengthening or/and precipitation strengthening, but addition of alloying elements deteriorates inevitably the thermal conductivity at the same instant due to the lattice distortion or/and formation of precipitates caused by alloying elements. For example, the thermal conductivity of cast AZ91 and AM60 is respectively about 58 [2] and $65 \text{ W}/(\text{m}\cdot\text{K})$ [3]. In addition, 3C products, shell of automobile engines and light emitting diode (LED) radiators demand both higher

mechanical and thermal properties [4], and thus the most frequently used cast Mg alloys such as AZ91 and AM 60 cannot meet the heat dissipation requirement of those products because of their low thermal and mechanical properties. The ultimate tensile strength (UTS) of AZ91 can be enhanced to 305 and 365 MPa from 125 MPa by multidirectional forging [5] and rolling [6], respectively. And the slow extrusion can increase the UTS of Mg-9Al alloy to 402 MPa [7]. The thermomechanical processes, however, simultaneously reduce the thermal property of the Mg alloys mainly due to much finer grain size and higher dislocation density of wrought Mg alloys than the cast alloys [8,9]. Therefore, it is necessary to develop new Mg alloys with a good combination of both thermal conductivity and mechanical properties for the wide applications of heat dissipation.

Since the different elements have the different effects on the mechanical properties [10–15] and thermal performance [2–4,16–22] of the Mg alloys, the alloying element type and concentration of the Mg alloys developed for the applications of heat dissipation should be carefully chosen in order to get a good balance between the thermal and mechanical properties. So far, most studies [2,3,9,16,17,19,20] have focused on the thermal conductivity of the Mg alloys without consideration from the angle of good combination of mechanical and thermal properties, which is undesirable for the applications of heat dissipation. It was reported that the cast Mg-Zn-Mn alloy exhibits the heat conductivity of 125 W/(m·K) [22] which is about twice as high as that of AZ91 and AM60, and the extruded Mg-Mn-Zn system alloys with a low content of Nd exhibit good strength [23]. Therefore, Mg-Mn-Zn-Nd alloys are expected to offer a good combination of thermal and mechanical properties. Until now, there has been no report on the thermal property of those Mg alloys. Thus, the thermal conductivity of Mg-Mn-Zn-Nd alloys was investigated to check if they are suitable for possible applications of heat dissipation.

2. Experimental

The fabrication and hot extrusion processes of designed Mg-1Mn-2Zn-xNd alloys ($x = 0.5, 1.0, 1.5$ wt. %) were detailed in the previous investigation [23]. The actual chemical compositions of designed Mg alloys, which were analyzed by X-ray fluorescence spectrometry, were shown in Table 1 [23]. The specimens with 10 mm (diameter) \times 3 mm (thickness) were machined from the cast ingots and extruded bars at cross section. The thermal diffusivity of the alloys was gauged at room temperature by laser flash method. The densities of the samples were calculated through Archimedes method and the Neumann–Kopp rule was used to determine the specific heat capacities of the designed alloys [24,25]. The thermal conductivity was obtained using the following equation [3]:

$$\lambda = \alpha \times \rho \times C_p \quad (1)$$

where α is thermal diffusivity (m^2/s), ρ is the density (g/cm^3) and C_p is the specific heat capacity ($\text{J}/(\text{g}\cdot\text{K})$) under constant pressure. The results were the averages of at least 3 sample tests.

Table 1. Chemical compositions of the Mg-1Mn-2Zn-xNd alloys (mass %).

Alloy Code	Mn	Zn	Nd	Ni	Fe	Al	Mg
Cast1	1.29	2.42	0.28	0.01	0.02	-	Bal.
Cast2	1.23	2.31	0.81	0.02	0.02	0.03	Bal.
Cast3	1.21	2.2	1.21	0.02	0.03	0.03	Bal.

Note: Cast1, Cast2, Cast3 respectively stand for the cast Mg-1Mn-2Zn-xNd alloys with Nd content of 0.5, 1.0 and 1.5%, and Extruded1, Extruded2, and Extruded3 stand for the extruded Mg-1Mn-2Zn-xNd alloys with Nd content of 0.5, 1.0 and 1.5%, respectively.

The phase constituents of the studied alloys were analyzed by X-ray diffraction analysis (XRD) operated at 40 kV and 40 mA with Copper $K\alpha$ radiation in $2\theta = 25\text{--}85^\circ$ and scanning speed of $0.02^\circ/\text{s}$. The microstructure of the designed alloys was observed by light microscopy (LM) and scanning electron microscope (SEM, Hitachi SU-1500) operated at 20 kV. The etching solution was composed of 5 mL nitric acid and 100 mL distilled water.

3. Results

3.1. Microstructure of the Alloys

The XRD results of the Mg-1Mn-2Zn-xNd alloys are presented in Figure 1 and Table 2. It is noticed that all the cast and extruded Mg alloys are composed of both α phase and Mg_7Zn_3 , and the extruded alloys exhibit the obvious texture because their strongest peaks are (100) which are different to the strong peaks (101) of the cast Mg alloys and powder Mg without texture (JCPDS card 35-0821). The slight increase of peak intensity of Mg_7Zn_3 suggests that the amount of Mg_7Zn_3 increases with addition of Nd content due to the limited solubility of alloying elements in α phase. The lattice parameters of α phase were calculated by software of Jade 6.0 based on the XRD results and summarized in Table 3. It can be seen that the c/a ratios of the crystal parameters of α phase slowly increase with Nd content, which causes larger crystal distortion and destroys the lattice periodicity.

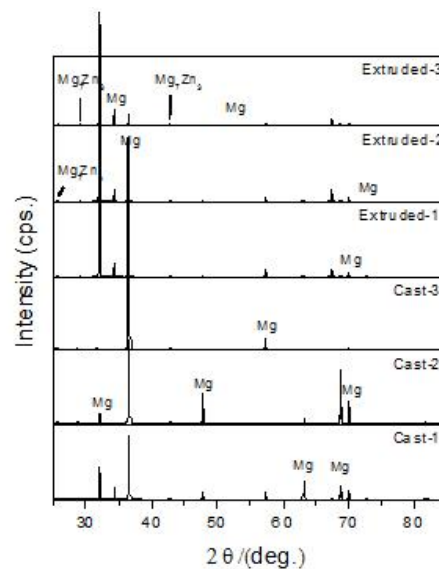


Figure 1. XRD patterns of the Mg alloys.

Table 2. Intensity of main peaks for α phase and Mg_7Zn_3 (cps.).

Alloy Code	A (100)	A (101)	Mg_7Zn_3 (400)	Mg_7Zn_3 (622)
Cast1	7842	86,119	905	978
Cast2	5493	41,023	990	1002
Cast3	3319	21,927	1090	1204
Extruded1	74,521	5027	1709	1678
Extruded2	74,255	5563	1909	1860
Extruded3	47,336	5828	2050	1969

Table 3. Lattice parameters of α phase and mean grain size of Mg alloys.

Alloy Code	Lattice Parameters			Grain Size
	a/nm	c/nm	c/a	μm
Pure Mg [26]	0.32094	0.52108	1.6236	–
Cast1	0.32095	0.52111	1.6236	200
Cast2	0.32088	0.52118	1.6242	155
Cast3	0.32097	0.52142	1.6245	100
Extruded1	0.32096	0.52130	1.6241	4~7
Extruded2	0.32107	0.52148	1.6242	4~7
Extruded3	0.32109	0.52156	1.6243	4~7

The microstructure of the cast Mg alloys is shown in Figure 2. The coarse equiaxed microstructure can be observed for all the cast Mg alloys, and their mean grain sizes measured by the method of linear intercept are 200, 155 and 100 μm , respectively, which indicates that the grain size of the Mg alloys slowly declines with addition of Nd content. On the contrary, all the extruded Mg alloys exhibit very fine microstructure with a mean grain size of 4~7 μm (Figure 3), which is due to the grain breakage caused by the hot-extrusion and recrystallization. It can also be observed that the number of white particles in Figure 3 increases with Nd content. In order to identify those white particles, the Energy Dispersive Spectrometer (EDS) was employed and the results are shown in Figure 4. The white particles are distributed in Mg-1Zn-1Mn-1.5Nd alloy as shown in Figure 4a. The EDS result in Figure 4b suggests that the white particle (assigned A area) should be Mg_7Zn_3 because the atom ratio of Mg/Zn is close to 7:3. Figure 4c indicates that the assigned area B (surrounding area of the white particles) is the α -Mg matrix. The finding is in agreement with the previous report [13,18,27].

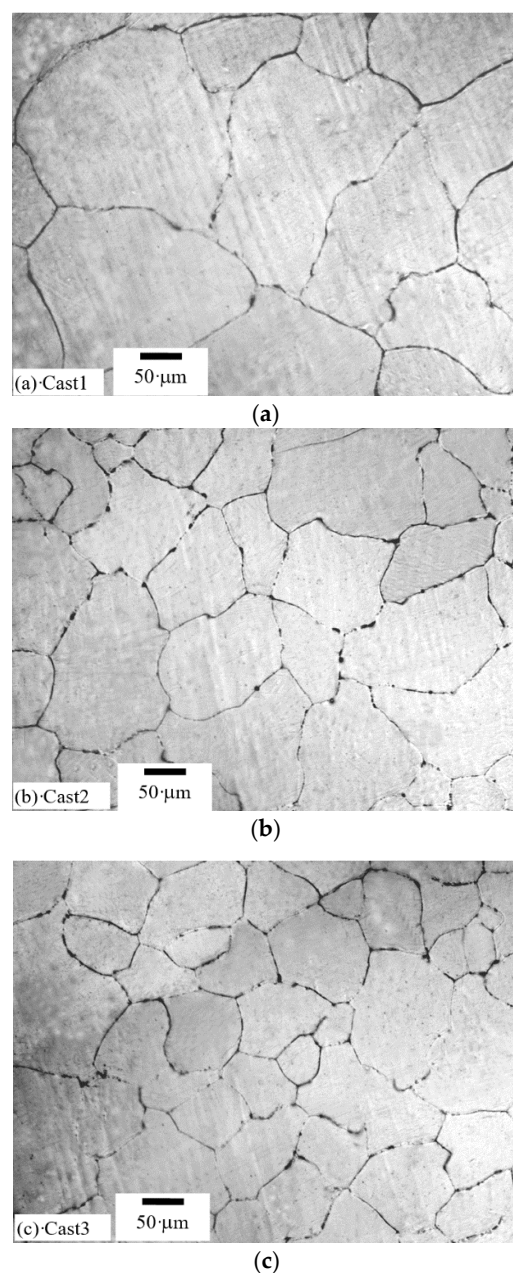
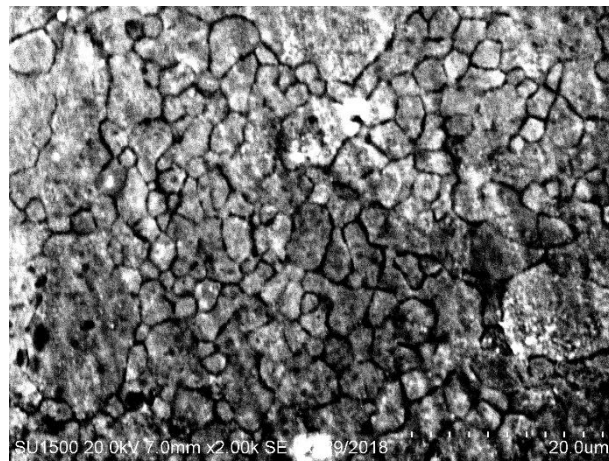
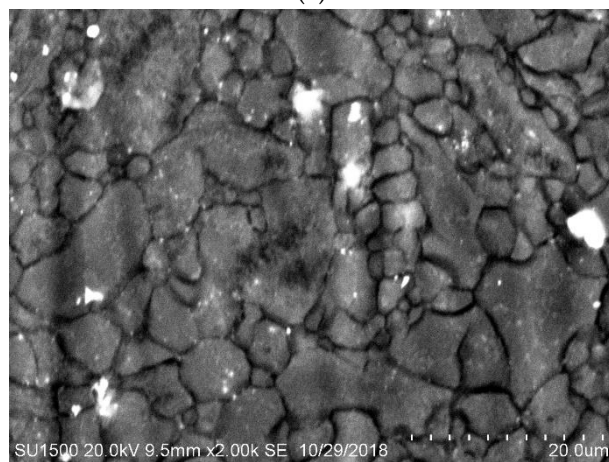


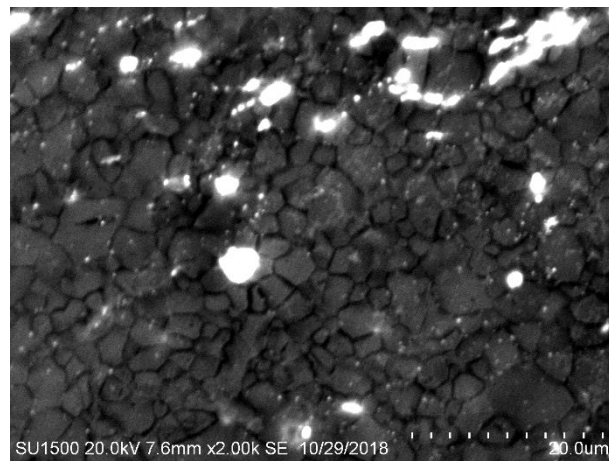
Figure 2. Light microscopy (LM) microstructure of the cast Mg alloys. (a) Cast1, (b) Cast2 and (c) Cast3.



(a)



(b)



(c)

Figure 3. SEM microstructure of the extruded Mg alloys. (a) Extrude1, (b) Extrude2 and (c) Extrude3.

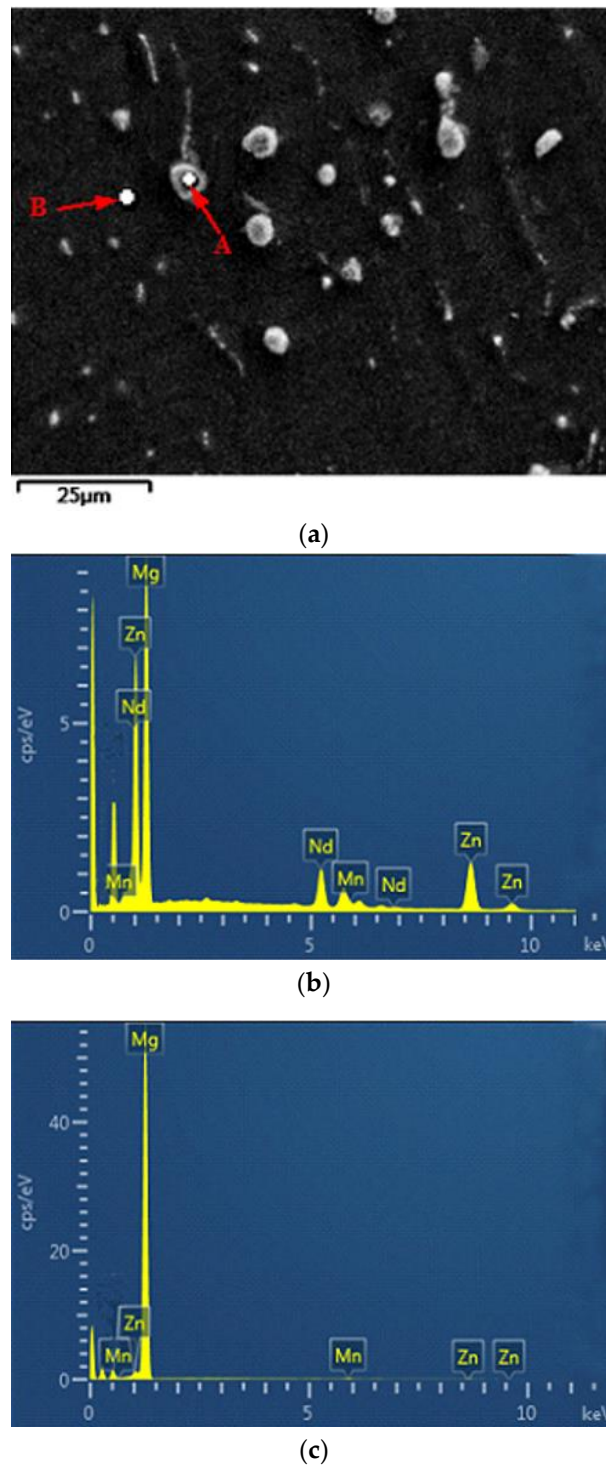


Figure 4. (a) SEM micrograph of the extruded alloy, (b) EDS analysis corresponding to assigned A area and (c) EDS analysis corresponding to assigned B area.

3.2. Thermal Conductivity

Figure 5 shows the thermal conductivity of the examined Mg alloys, which was calculated from the thermal diffusivity data using Equation (1). It can be observed that the thermal conductivity of both the cast and extruded Mg alloys slowly decreases with addition of Nd content, which is much lower than that of pure Mg (156 W/(m·K)). The thermal conductivity of the Mg alloys declines remarkably after the extrusion process. The standard deviation was less than 5%.

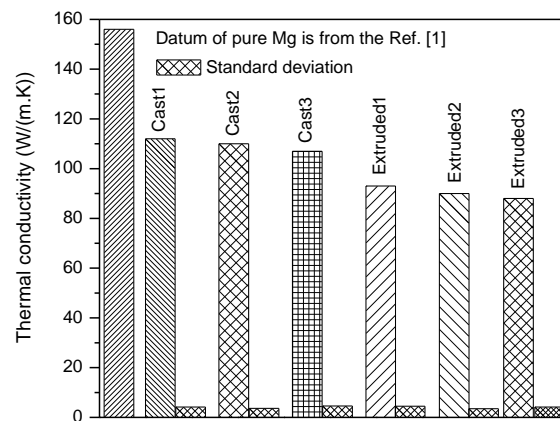


Figure 5. The thermal conductivity of the examined Mg alloys.

4. Discussion

4.1. Effect of Nd Content on the Thermal Conductivity

The electrons and phonons are the main heat carrier of the alloys, and the thermal conductivity is composed of electronic thermal conductivity and lattice thermal conductivity [28]. When the alloying elements dissolve in the α -Mg phase, the solid solutions will be formed and crystal lattice of the Mg matrix will be distorted. While the addition of alloying elements exceeds their solid solubility in α phase (Mg), precipitates are produced [12,13,23,27,29]. Solute atoms and precipitates, which are scattering centers of phonons and electrons, can reduce the mean free path of electrons and result in a reduction of the thermal conductivity of the alloy [4]. According to the above microstructure and Table 3, it can be considered that the increased lattice distortion, destruction of lattice periodicity and number of Mg_7Zn_3 particles (scattering centers), with addition of Nd content mainly account for the thermal conductivity of designed Mg alloys decreases with Nd content. The variation trend of thermal conductivity of the Mg alloys with alloy element content is in agreement with previous investigations [8,9,17,19,21,30].

4.2. Effect of Extrusion Process on the Thermal Conductivity

The lattice defects including vacancies, dislocations and crystal boundaries, are also the scattering centers of phonons and electrons that stop the free movement of electrons and accordingly reduce the thermal conductivity of the alloys [4,9]. The finer grain size leads to worse thermal performance of the Mg alloys [22,31]. As shown above (Figures 2 and 3), the extrusion process significantly reduces the mean grain size of the Mg alloys, so the extruded Mg alloys contain much more crystal boundaries (the scattering centers of phonons and electrons) than the cast alloys, which results in remarkable decreases of the thermal conductivity of the extruded alloys. This is the main reason why the extruded Mg alloys exhibit much lower thermal conductivity than the cast Mg alloys. As compared with the cast alloys, the extruded Mg alloys might contain a certain amount of dislocation caused by the extrusion, which also contributes to the reduction in the thermal conductivity of the extruded Mg alloys since the dislocation is also the scattering center of phonons and electrons and reduces the thermal conductivity of the extruded Mg alloys [31]. That the extruded Mg alloys exhibit lower thermal conductivity than the cast Mg alloys in this study is consistent with the previous investigations [8,9,18].

Texture may influence the thermal conductivity due to the anisotropic feature of Mg alloy with close-packed hexagonal structure [4]. Yuan et al. [18] investigated the thermal conductivity of extruded ZM51 in the extrusion and transverse directions, which was 110.7 and 117.9 W/(m·k), respectively. This indicates that the difference in the thermal conductivity between extrusion and transverse directions is about 6%, and the influence of the texture caused by extrusion process is relatively weaker as compared with the above factors such as alloying element and precipitates.

The strength of deformation texture generally depends on the processing method (rolling, extrusion or drawing), amount of deformation, deformation temperature, material nature and original state (original orientation). Larger deformation amount and lower deformation temperature usually leads to stronger texture. Since the Mg-1Mn-2Zn-xNd alloys in this study and the ZM51 [18], which were processed by the same method (extrusion), have the similar material nature and original state (homogenized), their difference in strength of texture is mainly related to the amount of deformation and deformation temperature. The extrusion ration (14.7) of the Mg-1Mn-2Zn-xNd alloys in this study is smaller than that (16) of the ZM51 [18] and the extrusion temperature (623 K) of the Mg-1Mn-2Zn-xNd alloys is higher than that (573 K) of the extruded ZM51 [18], thus the texture strength of the extruded Mg-1Mn-2Zn-xNd alloys should be weaker than that of the extruded ZM51 [18] and the influence of texture on the thermal conductivity of the Mg-1Mn-2Zn-xNd alloys is accordingly expected to be less than 6%.

The thermal conductivity of heat dissipation materials is an essential thermophysical performance. The more efficient cooling effect comes from the higher thermal conductivity [30], which can prevent the electric(al) equipment from overheating and prolong the service life. Huawei Technology Co., Ltd., a globe leading manufacturer of information and technology, demanded that the thermal conductivity of the cast and wrought Mg alloys should respectively exceed 100 and 120 W/(m·K) [31]. Thus, the cast Mg-1Mn-2Zn-xNd alloys exceed the required critical value (100 W/(m·K)) of thermal conductivity for the cast Mg alloys. The tensile properties of cast Mg-1Mn-2Zn-xNd alloy are shown in Table 4 [32] and it can be seen that the cast Mg-1Mn-2Zn-1Nd alloy exhibits the highest tensile strength of 185 MPa among the cast Mg alloys. Therefore, this alloy has a good combination of mechanical and thermal properties, and it has great potential to be a good candidate of heat dissipation materials. Although the extruded alloys have much higher strength [23] than the cast Mg alloys, their thermal conductivity is lower than the above critical value (120 W/(m·K)) for the wrought Mg alloys. Fortunately, recent studies have indicated that aging treatment can enhance the thermal performance of the Mg alloys [33–36]. Therefore, the thermal conductivity of extruded Mg-1Mn-2Zn-xNd alloys is expected to rise after aging treatment. Those experiments are under progress and the results will be reported later.

Table 4. Tensile properties of the cast Mg-1Mn-2Zn-xNd alloys.

Alloy Code	Ultimate Tensile Strength (MPa)	Tensile Yield Strength (MPa)
Cast1	181	55
Cast2	185	57
Cast3	110	41

5. Summary

The thermal conductivity of the Mg-1Mn-2Zn-xNd alloys ($x = 0.5, 1.0, 1.5$ wt. %) was studied for the potential applications of heat dissipation. The results show that the thermal conductivity of both the cast and extruded Mg alloys slowly decreases with addition of Nd content. The extrusion process remarkably reduces the grain sizes and thermal conductivity of the Mg alloys. The cast Mg alloys exhibit higher thermal conductivity than the critical value (100 W/(m·k)) of the as-cast Mg alloys required for the application of heat dissipation. The cast Mg-1Mn-2Zn-1Nd alloy has a great potential to be a good candidate of heat dissipation materials due to its good combination of mechanical and thermal properties.

Author Contributions: Investigation, Y.-L.Z., J.L., D.-M.L.; Data Curation, Y.-L.Z.; Writing-Original Draft Preparation, Y.-L.Z.; Writing-Review & Editing, J.L., D.-M.L., D.-C.C.; Visualization, Y.-L.Z., J.L.; Project Administration, Y.-L.Z., D.-C.C.; Funding Acquisition, Y.-L.Z., D.-C.C.

Funding: This research was funded by the Science and Technology Innovation Platform of Foshan City, Guangdong Province, China. (Grant No. 2014AG10009 and 2016AG100341).

Acknowledgments: The special gratitude was expressed to Lei Wang from Northeastern University, China for his kind help during the hot-extrusion process.

Conflicts of Interest: The authors declare no conflict of interest.

References

1. Hu, F.; Chen, Z. *Calorimetric Technology and Determination of Thermal Properties*; China University of Science and Technology Press: Hefei, China, 2009.
2. Yamasachi, M.; Kawamura, Y. Thermal diffusivity and thermal conductivity of Mg-Zn-rare earth element alloys with long-period stacking ordered phase. *Scr. Mater.* **2009**, *60*, 264–267. [[CrossRef](#)]
3. Rudajevová, A.; Staněk, M.; Lukáč, P. Determination of thermal diffusivity and thermal conductivity of Mg-Al alloys. *Mater. Sci. Eng. A* **2003**, *341*, 152–157. [[CrossRef](#)]
4. Peng, J.; Zhong, L.; Wang, Y.; Yang, J.; Lu, Y.; Pan, F. Effect of Ce addition on thermal conductivity of Mg-2Zn-Mn alloy. *J. Alloys Compd.* **2015**, *639*, 556–562. [[CrossRef](#)]
5. Nie, K.B.; Wang, X.J.; Deng, K.K.; Xu, F.J.; Wu, K.; Zheng, M.Y. Microstructures and mechanical properties of AZ91 magnesium alloy processed by multidirectional forging under decreasing temperature conditions. *J. Alloys Compd.* **2014**, *617*, 979–987. [[CrossRef](#)]
6. Wang, H.Y.; Zhang, E.B.; Nan, X.L.; Zhang, L.; Guan, Z.P.; Jiang, Q.C. A comparison of microstructure and mechanical properties of Mg-9Al-1Zn sheets rolled from as-cast, cast-rolling and as-extruded alloys. *Mater. Des.* **2016**, *89*, 167–172. [[CrossRef](#)]
7. Kang, J.; Sun, X.; Deng, K.; Xu, F.; Zhang, X.; Bai, Y. High strength Mg-9Al serial alloy processed by slow extrusion. *Mater. Sci. Eng. A* **2017**, *697*, 211–216. [[CrossRef](#)]
8. Ying, T.; Zheng, M.Y.; Li, Z.T.; Qiao, X.G. Thermal conductivity of as-cast and as-extruded binary Mg-Al alloys. *J. Alloys Compd.* **2014**, *608*, 19–24. [[CrossRef](#)]
9. Ying, T.; Zheng, M.Y.; Li, Z.T.; Qiao, X.G.; Xu, S.W. Thermal conductivity of as-cast and as-extruded binary Mg-Zn alloys. *J. Alloys Compd.* **2015**, *621*, 250–255. [[CrossRef](#)]
10. Khan, S.A.; Miyashita, Y.; Mutoh, Y.; Sajuri, Z.B. Influence of Mn content on mechanical properties and fatigue behavior of extruded Mg alloys. *Mater. Sci. Eng. A* **2006**, *420*, 315–321. [[CrossRef](#)]
11. Boehlert, C.J.; Knittel, K. The microstructure, tensile properties, and creep behavior of Mg-Zn alloys containing 0–4.4 wt.% Zn. *Mater. Sci. Eng. A* **2006**, *417*, 315–321. [[CrossRef](#)]
12. Cai, S.; Lei, T.; Li, N.; Feng, F. Effects of Zn on microstructure, mechanical properties and corrosion behavior of Mg-Zn alloys. *Mater. Sci. Eng. C* **2012**, *32*, 2570–2577. [[CrossRef](#)]
13. Zhang, E.; Yin, D.; Xu, L.; Yang, L.; Yang, K. Microstructure, mechanical and corrosion properties and biocompatibility of Mg-Zn-Mn alloys for biomedical application. *Mater. Sci. Eng. C* **2009**, *29*, 987–993. [[CrossRef](#)]
14. Zhang, X.; Meng, L.; Fang, C.; Peng, P.; Ja, F.; Hao, H. Effect of Nd on the microstructure and mechanical properties of Mg-Gd-5Y-2Zn-0.5Zr alloy. *Mater. Sci. Eng. A* **2013**, *586*, 19–24. [[CrossRef](#)]
15. Hu, G.; Zhang, D.; Tang, T.; Shen, X.; Jiang, L.; Xu, J.; Pan, F. Effects of Nd addition on microstructure and mechanical properties of Mg-6Zn-1Mn-4Sn alloy. *Mater. Sci. Eng. A* **2015**, *634*, 5–13. [[CrossRef](#)]
16. Pan, H.; Pan, F.; Yang, R.; Peng, J.; Zhao, C.; She, J.; Guo, Z.; Tang, A. Thermal and electrical conductivity of binary magnesium alloys. *J. Mater. Sci.* **2014**, *49*, 3107–3124. [[CrossRef](#)]
17. Zhong, L.; Peng, J.; Sun, S.; Wang, Y.; Lu, Y.; Pan, F. Microstructure and thermal conductivity of as-cast and as-solutionized Mg-Rare-Earth binary alloys. *J. Mater. Sci. Technol.* **2017**, *33*, 1240–1248. [[CrossRef](#)]
18. Yuan, J.; Zhang, K.; Li, T.; Li, X.; Li, Y.; Ma, M.; Luo, P. Anisotropy of thermal conductivity and mechanical properties in Mg-5Zn-1Mn alloy. *Mater. Des.* **2012**, *40*, 257–261. [[CrossRef](#)]
19. Wang, C.; Liu, Z.; Xiao, S.; Chen, Y. Effects of Sn, Ca additions on thermal conductivity of Mg matrix alloys. *Mater. Sci. Technol.* **2016**, *32*, 581–587. [[CrossRef](#)]
20. Rzychoń, T.; Kielbus, A. The influence of rare earth, strontium and calcium on the thermal diffusivity of Mg-Al alloys. *Defect Diffus. Forum* **2011**, *312*, 824–829. [[CrossRef](#)]
21. Oh, G.-Y.; Jung, Y.-G.; Yang, W.; Kim, S.K. Investigation of thermal conductivity and mechanical properties of Mg-4Zn-0.5Ca-Xy alloys. *Mater. Trans.* **2015**, *56*, 1887–1892. [[CrossRef](#)]
22. Yuan, J.; Zhang, K.; Zhang, X.; Li, X.; Li, T.; Li, Y.; Ma, M.; Shi, G. Thermal characteristics of Mg-Zn-Mn alloys with high specific strength and high thermal conductivity. *J. Alloys Compd.* **2013**, *578*, 32–36. [[CrossRef](#)]
23. Zhou, Y.-L.; Li, Y.; Luo, D.-M.; Ding, Y.; Hodgson, P. Microstructures, mechanical and corrosion properties and biocompatibility of as extruded Mg-Mn-Zn-Nd alloys for biomedical applications. *Mater. Sci. Eng. C* **2015**, *49*, 93–100. [[CrossRef](#)] [[PubMed](#)]

24. Leitner, J.; Voňka, P.; Sedmidubský, D.; Svoboda, P. Application of Neumann–Kopp rule for the estimation of heat capacity of mixed oxides. *Thermochim. Acta* **2010**, *497*, 7–13. [[CrossRef](#)]
25. Lindemann, A.; Schmidt, J.; Todte, M.; Zeuner, T. Thermal analytical investigations of the magnesium alloys AM 60 and AZ 91 including the melting range. *Thermochim. Acta* **2002**, *382*, 269–275. [[CrossRef](#)]
26. Magnesium: Crystal Structures. Available online: https://www.webelements.com/magnesium/crystal_structure.html (accessed on 9 November 2018).
27. Song, Y.; Han, E.-H.; Shan, D.; Yin, C.; You, B. The effect of Zn concentration on the corrosion behavior of Mg-xZn alloys. *Corros. Sci.* **2012**, *65*, 322–330. [[CrossRef](#)]
28. Berman, R. *Thermal Conduction in Solids*; Clarendon Press: Oxford, UK, 1976.
29. Liu, D.; Guo, C.; Chai, L.; Sherman, V.R.; Qin, X.; Dind, Y.; Meyer, M.A. Mechanical properties and corrosion resistance of hot extruded Mg–2.5Zn–1Ca alloy. *Mater. Sci. Eng. B* **2015**, *195*, 50–58. [[CrossRef](#)]
30. Rudajevová, A.; Von Buch, F.; Mordike, B.L. Thermal diffusivity and thermal conductivity of MgSc alloys. *J. Alloys Compd.* **1999**, *292*, 27–30. [[CrossRef](#)]
31. Peng, J.; Zhong, L.; Wang, Y.; Lu, Y.; Pan, F. Effect of extrusion temperature on the microstructure and thermal conductivity of Mg-2.0Zn-1.0Mn-0.2Ce alloys. *Mater. Des.* **2015**, *87*, 914–919. [[CrossRef](#)]
32. Zhou, Y.-L.; Li, Y.; Luo, D.-M. Effects of Nd on the microstructures, mechanical properties and in vitro corrosion behavior of cast Mg-1Mn-2Zn-xNd alloys. *Mater. Trans.* **2015**, *56*, 253–258. [[CrossRef](#)]
33. Pan, H.; Pan, F.; Peng, J.; Gou, J.; Tang, A.; Wu, L.; Dong, H. High-conductivity binary Mg–Zn sheet processed by cold rolling and subsequent aging. *J. Alloys Compd.* **2013**, *578*, 493–500. [[CrossRef](#)]
34. Huang, Q.; Tang, A.; Ma, S.; Pan, H.; Song, B.; Gao, Z.; Rashad, M.; Pan, F. Enhancing thermal conductivity of Mg-Sn alloy sheet by cold rolling and aging. *J. Mater. Eng. Perform.* **2016**, *25*, 2356–2363. [[CrossRef](#)]
35. Wang, C.; Cui, Z.; Liu, H.; Chen, Y.; Ding, W.; Xiao, S. Electrical and thermal conductivity in Mg–5Sn alloy at different aging status. *Mater. Des.* **2015**, *84*, 48–52. [[CrossRef](#)]
36. Li, B.; Hou, L.; Wu, R.; Zhang, J.; Li, X.; Zhang, M. Microstructure and thermal conductivity of Mg-2Zn-Zr alloy. *J. Alloys Compd.* **2017**, *722*, 772–777. [[CrossRef](#)]



© 2018 by the authors. Licensee MDPI, Basel, Switzerland. This article is an open access article distributed under the terms and conditions of the Creative Commons Attribution (CC BY) license (<http://creativecommons.org/licenses/by/4.0/>).